Published in final edited form as:

Arterioscler Thromb Vasc Biol. 2018 April ; 38(4): 913–926. doi:10.1161/ATVBAHA.117.310660.

Hypoxia Triggers SENP1 Modulation of Kruppel-Like Factor 15 and Transcriptional Regulation of Arginase 2 in Pulmonary Endothelium

Deepesh Pandey[1,*], **Yohei Nomura**[1], **Max C. Rossberg**[1], **Daijiro Hori**[1], **Anil Bhatta**[1], **Gizem Keceli**[5], **Thorsten Leucker**[5], **Lakshmi Santhanam**[1], **Larissa A. Shimoda**[6], **Dan Berkowitz**[1,3,#], **Lewis Romer**

[1]Department of Anesthesiology and Critical Care Medicine, Johns Hopkins Medical Institutions, Baltimore, MD 21287-4904

[2]Department of Cell Biology, Johns Hopkins Medical Institutions, Baltimore, MD 21287-4904

[3]Department of Biomedical Engineering, Johns Hopkins Medical Institutions, Baltimore, MD 21287-4904

[4]Department of Pediatrics, and the Center for Cell Dynamics, Johns Hopkins Medical Institutions, Baltimore, MD 21287-4904

[5]Divison of Cardiology, Johns Hopkins Medical Institutions, Baltimore, MD 21287-4904

[6]Division of Pulmonary and Critical Care Medicine, Department of Medicine, Johns Hopkins Medical Institutions, Baltimore, MD 21287-4904

Abstract

Objective—Kruppel-Like Factor 15 (KLF15) has recently been shown to suppress activation of proinflammatory processes that contribute to atherogenesis in vascular smooth muscle, however the role of KLF15 in vascular endothelial function is unknown. Arginase mediates inflammatory vasculopathy and vascular injury in pulmonary hypertension. Here we tested the hypothesis that KLF15 is a critical regulator of hypoxia-induced Arginase2 transcription in human pulmonary microvascular endothelial cells (HPMEC).

Approach and Results—Quiescent HPMEC express ample amounts of full length KLF15. HPMECs exposed to 24 hours of hypoxia exhibited a marked decrease in KLF15 protein levels and a reciprocal increase in Arg2 protein and mRNA. Chromatin immunoprecipitation indicated direct binding of KLF15 to the Arg2 promoter, which was relieved with HPMEC exposure to hypoxia. Furthermore, overexpression of KLF15 in HPMEC reversed hypoxia-induced augmentation of Arg2 abundance and arginase activity, and rescued nitric oxide (NO) production. Ectopic KLF15 also reversed hypoxia-induced endothelium-mediated vasodilatation in isolated rat pulmonary artery rings. Mechanisms by which hypoxia regulates KLF15 abundance, stability, and

[*]Address Correspondence to: Deepesh Pandey, Ph.D., Department of Anesthesiology and Critical Care Medicine, Johns Hopkins University; Baltimore, MD 21287-4904; Dpandey2@jhmi.edu.
[#]Contributed equally

Disclosures: None

compartmentalization to the nucleus in HPMEC were then investigated. Hypoxia triggered de-SUMOylation of KLF15 by sentrin-specific protease 1 (SENP1), and translocation of KLF-15 from nucleus to cytoplasm.

Conclusion—KLF15 is a critical regulator of pulmonary endothelial homeostasis via repression of endothelial Arg2 expression. KLF15 abundance and nuclear compartmentalization are regulated by SUMOylation/deSUMOylation – a hypoxia-sensitive process that is controlled by SENP1. Strategies including overexpression of KLF15 or inhibition of SENP1 may represent novel therapeutic targets for pulmonary hypertension.

Keywords

KLF15 Kruppel-Like Factor 15; Arg2 Arginase 2; SUMO Small Ubiquitin like modifiers; SENP1 Sentrin-Specific Protease 1; HPMEC Human Pulmonary Microvascular Endothelial Cells; Hypoxia; Transcriptional regulation

INTRODUCTION

Chronic hypoxia is a potent stimulus for pulmonary vasculature remodeling that progresses to Pulmonary Hypertension (PH)[1]. Accumulating evidence indicates that endothelial dysfunction is an early and critical event in the onset and progression of PH which is marked by danger signal receptor-mediated reduction in nitric oxide (NO) production and an increase in reactive oxygen species production[2]. Endothelial nitric oxide (eNOS) is a major target for the treatment of PH and its activity is controlled by a plethora of factors such as caveolin-1, HSP90, Akt-dependent phosphorylation and arginase 2 (Arg2). Although studies seem to converge on the reduction of NO production with hypoxia, effects of hypoxia on eNOS expression are inconsistent. For example, pulmonary arteries isolated from rats with hypoxia-induced PH exhibited either unchanged or increased expression of eNOS mRNA and protein as compared with controls, and increased eNOS protein expression has correlated positively with the development of PH in humans[2-6].

Our laboratory has been focused on factors that regulate the function of eNOS, but do not necessarily alter its abundance. Arg2 is an enzyme that has been conclusively demonstrated to reciprocally regulate the production of eNOS-derived NO and endothelial function[7-10]. Patients with PH have increased levels of lung HIF-1α[11,12], and hypoxia has been demonstrated as a robust stimulus for Arg2 expression in pulmonary artery endothelial cells by a mechanism involving transcriptional input from HIF-2α[13]. Indeed, HIF-2α has recently been shown to be a key transcription factor regulating pathogenesis of PH[14, 15]. However, HIF-2α is apparently not the only regulator of Arg2 in lung endothelium during hypoxia, and can only partly account for hypoxia-induced increases in Arg2 (Krotova, 2010, see figure 5 there[14]). These issues highlight the need for new targets in blood vessels for treatment or prevention of PH pathogenesis[16].

We have therefore taken a candidate approach to identify other important endothelial transcription factors that might regulate the expression of Arg2. The Kruppel- Like Factors (KLF) have been shown to be critical regulators of developmental and biological function in the vasculature, and are dysregulated in the context of endothelial pathobiology[17-20]. KLF2

and 4 are highly expressed in endothelial cells under laminar stress but their expression is significantly reduced at branch points and other areas of turbulent flow[21]. Moreover, KLF2 and 4 are important transactivators of eNOS, thereby contributing to laminar shear stress-induced increases in NO production and endothelial protection[22, 23]. Further, they lead to the repression of cytokine genes and increase the expression of adhesion molecules that inhibit endothelial cell inflammation and endothelial dysfunction. Importantly, hemizygous gene deletion of KLF2 and the myeloid-specific KLF4 gene deletion lead to accelerated atherogenesis in ApoE$^{-/-}$ mice[24, 25]. However, the recent elegant demonstration of reduction in plaque stability with smooth muscle cell-specific conditional knockout of KLF4 raises a concern regarding the strategy of activating KLF4 to treat atherogenesis[26]. KLF15 is a member of the KLF family that has garnered significant attention recently for its protective role in vascular inflammation and atherogenesis[27], proliferation and migration[28], heart failure and aortic aneurysm formation[29], and pressure-induced cardiac hypertrophy[30]. Although the importance of KLF15 is emerging in some cardiovascular diseases, the role of KLF15 in endothelial function is unknown.

At the outset of the current study, we aimed to determine the role of KLF15 in vascular endothelial function. We were intrigued by the almost complete loss of KLF15 expression in the cardiomyocytes of cardiomyocyte-specific ryanodine receptor type (tamoxifen-inducible) knockout mice, which has been shown to cause a hypoxia-like cellular state[31]. Hence, in the current work, we examined the role of KLF15 in controlling critical genes for vascular endothelial function in the context of hypoxia-induced pulmonary vascular disease.

MATERIALS AND METHODS

Reagents

All experimental procedures involving mice were approved by the Institutional Animal Care and Use Committee (IACUC) at The Johns Hopkins University School of Medicine. Rats were purchased from Jackson Laboratory. Unless otherwise stated, all reagents were obtained from Sigma. KLF15 siRNA was purchased from Qiagen. eNOS (sc-376542) and Arg2 (sc-20151) antibodies were purchased from Santa Cruz, KLF15 antibody was purchased from Novus biologicals (NBP2-24635). Anti-HA antibody (cat# 11867423001) was purchased from Roche (now Sigma-Aldrich). Alexa Fluor 488 anti-Rat secondary antibody was purchased from Invitrogen (Catalog # A-11094). KLF15 flexitube siRNA #7 (SI04184537), #9 (SI04299337) was purchased from Qiagen. Lipofectamine 2000 (Catalog# 11668027) was purchased from Life technologies. Live/Dead Viabiltiy/Cytotoxicity kit for mammalian cells was purchased from Thermofisher Scientific (catalog# L3224).

Cell culture

HPMEC were maintained in ECM culture medium (Science Cell Research Laboratories, Carlsbad, CA) according to the supplier's protocol. HPMEC were transfected using the Amaxa transfection system (Lonza). To subject cells to hypoxic environment, cell culture plates were inserted into hypoxic chambers, flushed with 5% CO2 and 95% Nitrogen for 10 min and the incubated in regular cell culture incubation with 5% CO_2.

RT-PCR and real time PCR

Total RNA was extracted from HPMEC using Trizol and PureLink (Invitrogen). RNA was then reverse transcribed with oligo dT primers to obtain cDNA and quantitative real time PCR (Applied Biosystems) was performed using SYBR Green Supermix mix (Applied Biosystems) whereas semi-quantitative RTPCR was performed using a conventional Biorad PCR machine and the following primer sets: *Human Arg2*: Forward: 5′-GGG CCC TGA AGG CTG TAG-3′, Reverse: 5′-AAT GGA GCC ACT GCC ATC-3′. *Human KLF15*: Forward: CCA AAA GCA GCC ACC TCA AG; REVERSE: GAC ACT GGT ACG GCT TCA CA. *Human KLF2*: Forward: 5′-CGG CAA GAC CTA CAC CAA GA-3′: Reverse: 5′- GCA CAG ATG GCA CTG GAA TG-3′ and *Human KLF4* Forward: 5′-AAG CCA AAG AGG GGA AGA CG-3′: Reverse: 5′-GCG AAT TTC CAT CCA CAG CC-3′.

Real Time PCR data are expressed as “fold change”, and is calculated as 2^-ΔΔCt. This is derived as follows: Delta Ct (ΔCt) means difference in Ct values between gene of interest (Arg2 in our case) and the housekeeping gene 18s; Delta Delta Ct (ΔΔCt) means difference in “Delta Ct” values between hypoxia and normoxia or GFP and KLF15 overexpression, and this is the ‘fold change’.

DNA constructs and Adenoviruses

HA- and FLAG-tagged KLF15 were constructed by PCR using untagged human KLF15 purchased from the Arizona State University plasmid repository as a template using and following primers: HA-KLF15-Forward-5′-GGG CCC GGA TCC ATG TAC CCC TAC GAC GTG CCC GAC TAC GCC GTG GAC CAC TTA CTT -3′; HA-KLF15-Reverse-5′GGG CCC CTC GAG CTA GTT CAC GGA GCG CAC GG-3′- -3′. 135 amino acids at KLF15 C-terminus corresponding to zinc-finger domain in KLF15 were truncated using following primers: Forward:5′-GGG CCC GAA TTC CTA AAT GCG CAC AAA CTT GGA GGG C-3′; Reverse:5′-GGG CCC GAA TTC CTA GTT CAC GGA GCG CAC GG-3′.

The PCR product was cloned into pcDNA3.1 using directional topo cloning (Invitrogen) Adenoviruses encoding HA and FLAG tagged KLF15 was constructed by subcloning into entry PENTR1a vector using and restriction enzymes followed by LR recombination with destination vector PDEST. The HDAC2-PDEST DNA was digested with PacI, ethanol precipitated and transfected into 293 HEK cells. After cytopathic effect (CPE), adenoviruses were collected and purified via three freeze-thaw cycles and a Millipore adenovirus purification Kit.

Generation of adenoviruses encoding shRNA

Ad-Nontargeted (Ad-Consh), Ad-KLF15sh and Ad-SENP1sh encoded viruses were generated using a pAdBLOCK-iT kit (Life Sciences). Briefly, oligonucleotides targeting 2 CDS region of Human KLF15 and SENP1 and non-targeted sequence were designed with proprietary software from Life Sciences and cloned into pU6-ENTR. Sequences used were as follows. Non targeted: Top,5′-CAC CGA TGG ATT GCA CGC AGG TTC TCG AAA GAA CCT GCG TGC AAT CCA TC-3′; Bottom, 5′-AAA AGA TGG ATT GCA CGC AGG TTC TTT CGA GAA CCT GCG TGC AAT CCA TC-3′. KLF15 shRNA-1:Top,5′-

CAC CGC ATC TTG GAC TTC CTA TTG TCG AAA CAA TAG GAA GTC CAA GAT GC-3′; Bottom,5′-AAA AGC ATC TTG GAC TTC CTA TTG TTT CGA CAA TAG GAA GTC CAA GAT GC-3′; KLF15 shRNA-2:Top,5′-CAC CGC CAG AAG TTT CCC AAG AAC CCG AAG GTT CTT GGG AAA CTT CTG GC-3′; Bottom,5′-AAA AGC CAG AAG TTT CCC AAG AAC CTT CGG GTT CTT GGG AAA CTT CTG GC-3′; SENP1 shRNA-1: Top, 5′- CAC CGC AGA ATA CTC TTG CAA TAC CCG AAG GTA TTG CAA GAG TAT TCT GC-3′; Bottom,5′- AAA AGC AGA ATA CTC TTG CAA TAC CTT CGG GTA TTG CAA GAG TAT TCT GC-3′; SENP1 shRNA-2: Top, 5′-CAC CGC ATT TCG CCT GAC CAT TAC ACG AAT GTA ATG GTC AGG CGA AAT GC-3′; Bottom, 5′-AAA AGC ATT TCG CCT GAC CAT TAC ATT CGT GTA ATG GTC AGG CGA AAT GC-3′. The resulting pU6-sh-Nontargeted and pU6-Arg2shRNA plasmids were tested for function in transient transfection experiments with 293A cells. The constructs showing the greatest inhibition were LR recombined with pAD/BLOCK-iTDEST (Invitrogen) to generate pAd-shKLF15 and pAd-shSENP1. Viruses were amplified and purified/concentrated using a Millipore Kit.

Force Tension Myography

Rat pulmonary artery (PA)was isolated and incubated in endothelia medium (ECM) either in normoxic or hypoxic conditions for 24h similar to cell culture conditions. Post 24h- PA was cleaned in ice-cold Krebs-Ringer-bicarbonate solution containing the following (in mM): 118.3 NaCl, 4.7 KCl, 1.6 $CaCl_2$, 1.2 KH_2 PO_4, 25 $NaHCO_3$, 1.2 $MgSO_4$, and 11.1 dextrose. The PA was immersed in a bath filled with constantly oxygenated Krebs buffer at 37°C. Equal size PA rings (2mm) were mounted using a microscope, ensuring no damage to the smooth muscle or endothelium. One end of the PA rings was connected to a transducer, and the other to a micromanipulator. PA was passively stretched to an optimal resting tension using the micromanipulator, after which a dose of 60 mM KCl was administered, and repeated after a wash with Krebs buffer. After these washes, all vessels were allowed to equilibrate for 20–30 min in the presence of indomethacin (3μM). Phenylephrine (1 μM) was administered to induce vasoconstriction. Dose-dependent responses (1nM to 10 μM), to the muscarinic agonist, ACH or to the nitric oxide donor, SNP, were then performed as necessary. The responses were repeated in the presence of inhibitors. Relaxation responses were calculated as a percentage of tension following pre-constriction. Sigmoidal dose-response curves were fitted to data with the minimum constrained to 0. Two to four rings were isolated from each animal and the number of animals in each group (n) was 6.

Human Arg2 promoter assay using luciferase activity

Chromosomal DNA was prepared from HPMEC using Trizol reagent as per manufacturer's protocol (Life sciences). Promoter fragments of Arg2 were amplified by PCR using genomic DNA isolated from HAEC and specific primer sets as follows: Arg2 promoter F: 5′-AAA CTC CTG ACC TCA GGT GA-3′, Arg2 promoter R: 5′-GCG GTT GGA AGC CGG GAG TG-3′. The PCR product was used as a template to further add XhoI and HIndIII sites to the 5′ and 3′ end respectively using following primers: Arg2 Xho-5′-GGG CCC CTC GAG AAA CTC CTG ACC TCA GGT GAT CCA CCT GCC TC-3′ and Arg2 HindIII-5′-GGG CCC AAG CTT GCG GTT GGA AGC CGG GAG TGA GCG CCA CCG CCC G-3′. These were cloned into the restriction sites for XhoI and HindIII on the pGL3-enhancer vector

(Promega Co.). HPMEC were transfected with the plasmids using Fugene 6 reagent (Roche Co.) and luciferase activity was measured by Dual-luciferase reporter assay system (Promega Co.). The luciferase activity was reported as relative luciferase units by dividing firefly luciferase activity by Renilla luciferase activity and normalized to protein concentration.

Transcription factor (TF) binding consensus sequences in Arg2 promoter sequence were analyzed by using Ensembl, TRANSFAC database (http://www.gene-regulation.com/pub/databases.html#transfac) and MacVector software (Accelrys, San Diego, CA).

Immunoprecipitation and Western blotting

After 48hrs of HPMEC cells transfection, cells were lysed in ice cold RIPA lysis buffer consisting of 20 mM Tris–HCl at PAH 7.5, 150mM NaCl, 1mM EDTA, 1mM EGTA, 1%NP40, 1% sodium deoxycholate, 1 mM Na_3VO_4, 2.5mM sodium pyrophosphate, 1mM β-glycerophosphate, 1μg/mL leupeptin, and a 1:1000 diluted protease inhibitor cocktail (Sigma). For immunoprecipitation studies, whole cell lysate lysates were centrifuged at 14,000 × g and supernatants were precleared by incubation with Protein A/G-agarose beads for 2 h at 4° C with rocking. Agarose beads were then pelleted by centrifugation at 1,000 × g. FLAG-Arg2 in precleared lysates were immunoprecipitated by incubation overnight at 4° C with rocking following addition of anti-FLAG antibody (10 μl). Immune complexes were eluted in 2x SDS sample buffer by boiling for 5 minutes before loading into SDS–PAGE. Western blotting analysis was performed by transferring the SDS gel onto a PVDF membrane and visualized using secondary antibodies conjugated to alkaline phosphatases.

Arginase activity assay

HPMEC were lysed using RIPA buffer (50 mM of Tris.HCl, PAH 7.5, 0.1 mM EDTA, 0.1% Triton X-100, and protease inhibitor), and centrifuged for 30 min at 14,000 g at 4°C. 50 μL (50-100μg) of supernatant was added to 75μl of 10 mM $MnCl_2$ made in Tris-HCl (50 mM, PAH 7.5) and heat activated by incubating at 55-60°C for 10 min. 50 μL of L-Arginine that was prepared in 300mM Tris-HCL, PAH 9.7 were then added to the activated cell lysates to achieve final concentrations of 150mM and incubated at 37°C for 3 hrs with shaking. The reaction was stopped by adding 400 μL of an acid solution (H_2SO_4: H_3PO_4: H_20=1:3:7). For colorimetric determination of urea, α-isonitrosopropiophenone (25 μL, 9% in ethanol) was added and further heated at 100°C for 45 min. Samples were allowed to cool at room temperature in the dark for 10 min and urea concentration was determined by measuring absorbance at 550nm using a spectrophotometer.

Subcellular localization

Subcellular localization of KLF15 in response to hypoxia was determined by immunofluorescence. Briefly, upon conclusion of hypoxia, HPMECs were permeabilized for 2 minutes with 0.5% Triton X-100 (Sigma Aldrich) in 4% paraformaldehyde solution. Cells were then fixed in 4% paraformaldehyde for 20 minutes at room temperature followed by 2 washes with PBS. Samples were incubated with anti-HA antibody (Sigma-Aldrich, rat, 1:100) in blocking buffer (0.1% BSA in Universal Buffer) for 1 hour at 37°C. Samples were then incubated in secondary antibody (Alexafluor 488 anti-rabbit secondary antibody, 1:100

dilution, Invitrogen) and DAPI for 1 hour at 37°C. Samples were subsequently mounted with FluorSave™mounting medium (EMD Millipore). Images were acquired using Zeiss LSM 800 laser-scanning confocal microscope equipped with Zen 2.3 software (2011).

Chromatin Immunoprecipitation (ChIP)

ChIP was performed using Magna ChIP kit from Millipore as per manufacturer's protocol. Briefly, Confluent HPMEC expressing HA-KLF15 were incubated with 1% formaldehyde at 37°C for 10 minutes to crosslink Histones and DNA. The crosslinked complexes were subjected to shearing with sonication and immunoprecipitated with anti-HA antibody. After reverse crosslinking, purified and immunoprecipitated DNA was amplified using real time PCR and Arg2 promoter-specific primers: CHIP-A For: 5′-TTC AAT GAA CTG AAC AAG TAT G-3′; CHIP-A Rev: 5′-TAG GGC ACC GGT AAC CTA TG-3′, CHIP-B For: 5′-TTG GCC TTC TGG CGT CAG CG-3′: CHIP-B Rev: 5′-GCT CTG CAA GGC TGG GAC GTG-3′.

Measurements of nitric oxide production

Nitric Oxide production in the cell culture media was determined by measuring nitrite levels with a Siever's NO analyzer. Nitric oxide levels in HPMEC were also determined using DAF-DA as per manufacture instructions (Life Sciences). Briefly, cells were loaded with DAF-DA (5 μM) for 20 min and washed 3 times with PBS and incubated for another 30 min in phenol-free media. Fluorescence was determined using a Nikon TE-200 epifluorescence microscope. Images were captured with a Rolera EMC2 camera (Q-Imaging, BC, Canada) with Velocity software (PerkinElmer, Lexington, MA).

Meaurements of reactive oxygen species production

Luminol analog L-O12[32] as described previously and EPR was used to measure ROS. Briefly, HPMEC overexpressing either GFP or HA-KLF15 were incubated under normoxic or hypoxic conditions for 24h. Post -24h, cells were treated with 0.075 mL phosphate-buffered saline (PBS) containing 0.1 mM diethylenetriaminepentaacetic acid (DTPA) and protease inhibitor cocktail (Roche Applied Science, Indianapolis, IN) at pH 7.4. The cells were scraped, kept on ice, and analyzed within 1 h. Stock solutions of 1-hydroxy-3-methoxycarbonyl-2,2,5,5-tetramethylpyrrolidine hydrochloride (CMH; Enzo Life Sciences, Farmingdale, NY) were prepared daily in nitrogen purged 0.9% (w/v) NaCl, 25 g/L Chelex 100 (Bio-Rad) and 0.1 mM DTPA, and kept on ice[1]. The samples were treated with 1 mM CMH at RT for 10 min, transferred to 0.050 ml glass capillary tubes, and analyzed on a Bruker E-Scan (Billerica, MA) electron paramagnetic resonance (EPR) spectrometer. Spectrometer settings were as follows: sweep width=100 G; microwave frequency=9.75 GHz; modulation amplitude=1 G; conversion time=5.12 ms; receiver gain=2×10^3; number of scans=16.

Stretching Protocol

HPMECs were uniaxially stretched (15%, 1Hz) using a stretching apparatus (ST-140-10; STREX, Osaka, Japan) for 6 hours. Cell media were collected from the stretch chambers for nitrite measurements using Siever's.

Sugen-Hypoxia Protocol

Rats were subcutaneously injected with SU5416 (20 mg/kg) and placed in a chamber maintained at FiO_2=10% for 21 days. Control normoxic rats remained next to the chamber to maintain consistent environmental factors. At day 21, rats were removed from hypoxia, anesthetized with pentobarbital via intra-peritoneal injections and lungs were explanted. The lungs were instilled with 10% formalin, removed en bloc and fixed in formalin prior to embedding and sectioning. The sections were subjected to immunohistochemical staining using KLF15 antibody.

Statistics

All statistical analyses were performed using Prism 7 for Mac, by GraphPad Software Inc., and by Microsoft Excel version 14.1.3 statistical analysis software. The results were expressed as mean and standard error (mean ± SEM). One-way analysis of ANOVA and the Bonferroni post-hoc test for multiple-comparison were used to compare all experimental data sets, groups, and pairs of data sets, respectively. A value of $p < 0.05$ was considered statistically significant. Myograph data were analyzed using general linear model with group as a factor and dose as a repeated measure using STATA VERSION 15 software, STATA Corporation, College Station, TX. Post-hoc tests were applied for each dose using linear combination based on this model.

RESULTS

KLF15 is expressed in quiescent human pulmonary microvascular endothelial cells, and regulates expression of Arg2 and eNOS - enzymes that are critical for endothelial function

Recent studies that were focused primarily on vascular smooth muscle cells suggested an important role for KLF15 in vascular injury, inflammation and atherosclerosis[28, 29, 33]. We therefore investigated the role of KLF15 in the regulation of genes that affect pulmonary vascular endothelial function. We first determined whether KLF15 mRNA was expressed in human pulmonary microvascular endothelial cells (HPMEC). As shown in Figure 1A, using RT-PCR we demonstrated that KLF15 mRNA is expressed in substantial quantities in HPMEC. These data provide the first evidence for the expression of KLF15 in endothelial cells. We compared KLF15 expression in human endothelial cells cultured from different vascular beds (pulmonary microvascular, aortas and coronary artery) to expression in human aortic smooth muscle cells (HASMC). As shown in Figure 1B, KLF15 was expressed at varying levels in endothelial cells isolated from all 3 endothelial populations. Cell lysates of ectopically expressed FLAG-KLF15 were used as a positive control for KLF15 expression. Interestingly, it appears that HASMC express KLF15 at much lower levels than endothelial cells (Figure 1B). We also measured and compared relative levels of KLF15 to KLF2 and KLF4 - transcription factors that are well-studied in the context of endothelial function[19]. KLF15 expression was found to be significantly higher in HPMEC than that of either KLF4 or KLF2 (Figure 1C). As a transcription factor and a regulatory protein, it's expression level was however found to be lower than that of the highly abundant EC proteins and markers CD31 and VWF (Supplemental Figure I). Arg2 and eNOS compete for L-arginine, and Arg2 reciprocally regulates eNOS and the production of NO that is protective for endothelium[34]. In the systemic circulation, Arg2 expression is enhanced during atherogenesis, resulting in

endothelial dysfunction by uncoupling eNOS[8, 35, 36]. Transient overexpression of KLF15 in quiescent HPMEC robustly increased eNOS levels and almost completely obliterated Arg2 protein levels (Figure 1D). This effect was found to be dose-dependent (data not shown). Increased KLF15 expression also attenuated arginase activity in quiescent HPMEC and increased NO production (Figure 1, E and F-bottom panel). Furthermore, the observed KLF15-mediated increase in nitric oxide production was enhanced when cells were subjected to physiologic stretch in a pattern that mimicked human breathing parameters[37] as shown in Figure 1F-top panel. We next determined whether loss of KLF15 function in HPMEC has any effect on Arg2 levels. Using 2 different siRNAs (#7, #9) targeted to two different regions of KLF15 coding DNA sequence (CDS), we demonstrated that KLF15 knockdown resulted in 4-6 fold increase in Arg2 levels (Figure 1G).

KLF15 is decreased by hypoxia in HPMEC

We exposed HPMEC to hypoxia (2% O_2) to test the effects of this stimulus on KLF15, and found that protein levels were markedly reduced, but that mRNA levels were unchanged (Figure 2A, 2B, 2G, 4th panel and Supplemental Figure II). This reduction in KLF15 was maintained through 24 hours of reoxygenation (Supplemental Figure II). Additionally, exposure of cells to mild hypoxia (8% O_2) also resulted in reduction of KLF15 abundance and a reciprocal increase in Arginase 2 (Supplemental Figure IV, A-B). In contrast, endothelial cells from human aortas and coronary arteries did not exhibit hypoxia-mediated reduction in KLF15 abundance, despite the fact that hypoxia induced increased Arg2 levels in these cells. This indicates that KLF15 sensitivity to hypoxia is unique to HPMEC (among the EC studied thus far) (Supplemental Figure V). Using immunohistochemistry (Figure 2C) and western blot (Figure 2D) we further demonstrated that KLF15 abundance is significantly reduced in pulmonary artery (PA) of rats exposed to combination protocol involving Sugen (VEGF receptor antagonist) and chronic hypoxia, as described in method section. Quantitative analyses are presented in the upper panel of the representative images. Using a live/dead cell assay kit (Life technologies) we demonstrated hypoxia caused no significant effect on HPMEC viability (Supplemental Figure IIIA). Endothelial cells express two isoforms of arginase, Arg1 and Arg2. Hypoxia induced large increases in Arg2 protein and mRNA levels, as well as in arginase activity (Figure 2, E-K), but Arg1 levels were unchanged by either hypoxia or transient overexpression of KLF15 (Figure 2G, 2nd panel). Hypoxia failed to reduce eNOS levels in HPMEC (Figure 2G, 3rd panel). These finding strongly suggested that hypoxia-mediated endothelial dysfunction occurred through eNOS uncoupling by upregulated Arg2 levels rather than via either a reduction in eNOS abundance or by Arg1-mediated regulation. To determine whether the zinc finger domain of KLF15 located at the C-terminus is critical for the inhibitory effect of KLF15 on hypoxia-induced Arg2 expression, we studied HPMEC expressing either full length KLF15 or KLF15 with a truncated C-terminal zinc finger domain (135 amino acids) via adenoviral delivery, in either hypoxia or normoxia. Induction of Arg2 by hypoxia was completely blocked in HPMEC that ectopically expressed full length KLF15 whereas the truncated KLF15 had no effect (Figure 2H). Further, HPMEC overexpressing KLF15 exhibited ablation of increases in arginase activity in response to hypoxia (Figure 2I). In contrast, genetic knockdown of KLF15 by siRNA or shRNA (the effectiveness of Ad-shRNA is shown in Supplemental Figure XI) augmented these responses to hypoxia (Figure 2J, and 2K). Notably, overexpression of either

KLF2 or KLF4 had minimal effects on Arg2 levels in HPMEC under either hypoxic or normoxic conditions (Figure 2G).

KLF15 over-expression reverses Arg2-mediated effects of hypoxia on HPMEC NO and ROS production

To determine whether KLF15 confers protection against hypoxia-induced endothelial dysfunction, we measured NO and superoxide in HPMEC overexpressing either GFP (control) or KLF15 during normoxic and hypoxic conditions. As expected, hypoxia significantly reduced NO and increased ROS production in HPMEC (Figure 2L, 2M and Supplemental Figure VI). Overexpression of KLF15 in HPMEC completely reversed hypoxia-induced attenuation of NO production, and also reduced levels of ROS (Figure 2L and 2M). Further, HPMEC co-expressing both KLF15 and Arg2 produced about one half as much NO during hypoxia as cells that overexpressed KLF15 alone. This suggests that Arg2 is a critical gene target for KLF15 in hypoxia (Figure 2L).

Impairment of endothelial-dependent pulmonary artery relaxation by hypoxia is ameliorated by KLF15 overexpression

The significant protection offered by KLF15 against hypoxia-induced increased ROS and reduced NO production in HPMEC prompted us to explore whether these cellular events translated to physiological function at the whole tissue (blood vessel) level. We determined the effects of hypoxia on acetylcholine-dependent relaxation in isolated rat pulmonary artery segments with intact endothelium. Hypoxia significantly impaired endothelium-dependent relaxation in rat pulmonary artery (Figure 3A) without affecting endothelium-independent relaxation (response to sodium nitroprusside) (Figure 3B). Impaired endothelial-dependent relaxation during hypoxia was almost completely reversed in pulmonary arteries following transduction with adenoviruses encoding KLF15 (Figure 3A). KLF15 levels in transduced and non-transduced pulmonary arteries are shown in Figure 3C. To determine whether the adenoviral transduction of the pulmonary artery explants induced endothelial cell-specific increases in KLF15 expression, pulmonary artery rings that had the endothelium denuded were studied in parallel with intact vessels. PA segments demonstrated near-total abolition of KLF15 expression following denuding of the vascular endothelium. CD31 serves as a positive control for endothelial cells in this experiment.

KLF15 acts as a transcriptional repressor of Arginase 2 by binding to its promoter, a process that is reversed by hypoxia

To explore the mechanism by which KLF15 regulates Arg2, we determined whether transient overexpression of KLF15 in HPMEC altered Arg2 transcription. Using RT-PCR and Arg2-specific primers, we found that Arg2 mRNA expression was down-regulated by increased expression of KLF15 (Figure 4, A and B). Importantly, KLF15 overexpression had no effect on ectopic expression of GFP-tagged Arg2 that was controlled by an artificial cytomegalovirus (CMV) promoter (Figure 4C). Additionally, a cycloheximide (inhibitor of *de novo* protein synthesis) chase assay was performed to determine whether a drop in Arg2 protein levels by KLF15 overexpression was due to shortening of the half-life of Arg2 protein by increased KLF15 expression. As shown in Figure 4, this seems to be an unlikely explanation (Figure 4D). These results suggest that KLF15 is involved in transcriptional, but

not translational regulation of Arg2. To determine whether hypoxia regulates Arg2 promoter activity, and whether KLF15 overexpression may modulate this effect, we co-transduced KLF15 and an Arg2 promoter-luciferase reporter construct using adenoviruses in HPMEC exposed to normoxia or hypoxia. Luciferase activity generated by the Arg2 promoter was substantially higher in cells grown in hypoxic conditions, and this upregulation of Arg2 promoter activity by hypoxia was absent in HPMEC overexpressing KLF15 (Figure 4E).

We next investigated the possibility that KLF15 interacts directly with the Arg2 promoter. We identified 2 consensus KLF-binding sequences - CACCC and GGGTG - within the 2kb region of the Arg2 promoter that is upstream of the transcription start site (Supplemental Figure VIII). A chromatin immune precipitation assay (ChIP), using anti-HA antibody and primers spanning Arg2 promoter segments containing these consensus KLF15-binding sequences, demonstrated that KLF15 binds to both the proximal and the distal regions of the Arg2 promoter (Figure 4F). KLF15 binding to the distal promoter region was found to be much higher. Moreover, hypoxia disrupted binding of the Arg2 promoter by KLF15. The greater interaction that we observed between KLF15 and the distal (vs the proximal) Arg2 promoter was consistent with the lower basal promoter activity of the distal Arg2 promoter segment as compared with that of the proximal segment (Figure 4G). In response to hypoxia, the activities of both Arg2 promoter segments were enhanced - yet notably, the distal promoter exhibited greater augmentation by hypoxia (Figure 4H and 4I). Taken together, these data provide direct evidence that KLF15 is a transcriptional repressor of hypoxia-induced Arg2 expression.

KLF15 is ubiquitinated and hypoxia accelerates proteasomal degradation of KLF15

We next investigated mechanism(s) by which hypoxia might downregulate protein (but not mRNA) levels of KLF15 in HPMEC (see Figures 2A, 2B, 2E and 5A). Pre-treatment of HPMEC with the proteasomal inhibitor-MG132 not only reversed the effects of hypoxia, but increased KLF15 above control levels (5A). This finding suggested that ubiquitin-directed degradation could play a critical role in hypoxia-mediated decreases in KLF15. Next, FLAG-KLF15 and either GFP alone or HA-ubiquitin were co-expressed in HPMEC. Co-immunoprecipitation with an anti-FLAG antibody and immunoblotting with an anti-HA antibody were then performed. High molecular weight bands (a hallmark of ubiquitinated proteins) were found in lysates from cells co-expressing KLF15 and ubiquitin, but not in cells co-expressing KLF15 and GFP (control plasmid) (Figure 5B). Hypoxia greatly upregulated KLF15 ubiquitination (Figure 5C). To determine the physiologic relevance of proteasomal degradation of KLF15, the proteasome inhibitor bortezomib was studied in isolated rat PA vasoreactivity in normoxic and hypoxic conditions (Supplemental Figure VII, A and B). Bortezomib pretreatment protected EC-dependent vasorelaxation in hypoxia. These findings suggest that hypoxia enhances ubiquitination of KLF15, and targeting of KLF15 for proteasomal degradation.

KLF15 is a SUMO-1 substrate and is de-SUMOylated during hypoxia

Since KLF15 is a transcription factor that resides primarily in the nucleus, its availability for hypoxia-enhanced ubiquitin-mediated clearance implies that it is first translocated to the cytoplasm. We evaluated whether KLF15 is a SUMO-1 substrate because SUMO-1

modification of proteins have a a role in nuclear localization and export[38]. HPMEC were transduced with HA-tagged KLF15 together with one of the following: an active mutant of GFP-tagged SUMO-1 that has exposed di-glycine residues at its C-terminus; an inactive mutant of GFP tagged SUMO-1 that lacks di-glycine residue at the C-terminus making it incapable of forming a disulfide link with its substrate (Supplemental Figure IX); or GFP alone (control plasmid). As shown in Figure 5D, a higher molecular weight band consistent with SUMO1+GFP (35kDa) binding to KLF15 was seen in addition to unmodified HA-KLF15 in lysates from HPMEC co-expressing KLF15 and constitutively active SUMO-1. In contrast, lysates from HPMEC co-expressing KLF15 and inactive SUMO-1 or GFP alone did not exhibit this higher MW band. This indicates that the higher HA-KLF15 bands represented covalent conjugation of SUMO1 to KLF15. We next determined whether hypoxia modulates SUMOylation of KLF15, and found that the amount of SUMOylated KLF15 was indeed attenuated in HPMEC that were exposed to 2 hours of hypoxia, a time consistent with post-translational modification (Figure 5E). KLF15 levels in HPMEC co-expressing KLF15 and SUMO were consistently higher than those observed in HPMEC expressing KLF15 and GFP. This prompted us to investigate the effects of SUMOylation on the stability of KLF15 levels. Cycloheximide chase experiments in HPMEC co-expressing either KLF15 and GFP or KLF15 and SUMO1 demonstrated higher and sustained levels of KLF15 in the presence of SUMO-1 (Figure 5H).

KLF15 primarily resides in the nucleus in quiescent HPMEC, and is translocated to the cytoplasm during hypoxia

To determine whether hypoxia-induced Arg2 expression in HPMEC involves translocation of its transcriptional repressor, KLF15 from nucleus to cytoplasm, we exposed HPMEC expressing HA-KLF15 to hypoxia and monitored KLF15 localization using HA antibody and cell fractionation. In a quiescent HPMEC, KLF15 was found primarily localized to the nucleus, but 2 hours of hypoxia triggered translocation of KLF15 from the nucleus to the cytoplasm (Supplemental Figure X).

SENP1 mediates hypoxia-dependent induction of endothelial Arg2 by deSUMOylating and affecting subcellular localization of KLF15

As SUMOylation is a dynamic process that is catalyzed by SUMO- specific ligases and reversed by SUMO specific proteases, we next determined whether the deSUMOylating enzyme, SENP1, and the SUMO-specific ligase, PIASγ-E3 ligase, can modulate KLF15 SUMOylation. As shown in Figure 6A, increased expression of GFP-tagged SENP1 obliterated SUMOylated KLF15 while knockdown of SENP1 with shRNA robustly induced KLF15 SUMOylation. This effect appears to be dose-dependent (Figure 6A). The effectiveness of our reagents in achieving SENP1 overexpression and knockdown is demonstrated in Supplemental Figures XII and VIII, respectively. Further, increased expression of SUMO-specific ligase PIASγ significantly upregulated SUMO-modified KLF15 (Figure 6B). We next determined the effect of SENP1 interference on hypoxia-induced Arg2 expression in HPMEC. As shown in Figure 6C-D, increased expression of SENP1 potentiated, whereas silencing SENP1 (Figure 6D-E) significantly attenuated, the Arg2 levels induced by hypoxia. The effectiveness of SENP1 knockdown is demonstrated by dramatic upregulation in global SUMOylation (Figure 6D, 2nd panel). One of the critical

consequences of SUMO modification is altered subcellular localization of substrate proteins[39]. To determine whether hypoxia-driven translocation of KLF15 from the nucleus to cytoplasm is mediated by SENP1, we exposed HPMEC co-transduced with HA-KLF15 with either scrambled shRNA or SENP1 shRNA and subject them to either normoxic or hypoxic condition. As shown in Figure 6F-G and Supplemental Figure X, A-C, KLF15 was primarily localized in nucleus in HPMEC transduced with scrambled shRNA that were cultured in normoxic conditions. This changed within two hours of exposure to hypoxia, after which a substantial amount of KLF15 was found to be cytosolic (Figure 6F-G and Supplemental Figure X, A-C). In contrast, hypoxia failed to de-compartmentalize KLF15 from the nucleus to the cytoplasmic fractions in HPMEC that were transduced with SENP1-shRNA (Figure 6G).

DISCUSSION

Our finding that protein levels of KLF15 are responsive to hypoxia in pulmonary microvascular endothelium provides new insight into transcriptional control of functional homeostasis in the lung microcirculation and its derangement by hypoxia. Transcriptional repression of Arg2 by KLF15 is apparently an important component of the regulatory landscape in normal pulmonary endothelium, and prevents the deleterious constellation of consequences that are triggered by induced Arg2 expression: blunted nitric oxide release; increased reactive oxygen species production; and impaired endothelium-dependent vascular relaxation (Figures 1-4)[8, 36]. Further, data presented here delineate the molecular mediation of hypoxia-mediated alteration of subcellular localization of KLF15, and a decrease in its availability in microvascular lung endothelium. These occur by way of SENP1-mediated de-SUMOylation of nuclear KLF15, translocation of KLF15 to the cytoplasm, and acceleration of ubiquitin-proteasome-mediated degradation and clearance of KLF15 (Figures 5 and 6). Diminished KLF15 levels release a transcriptional brake on Arg2, resulting in vascular dysfunction. These mechanisms are summarized in the schematic presented in Figure 7.

Although pulmonary endothelial function has been implicated heretofore in hypoxia-induced PAH, studies have focused largely on hypoxia inducible factor (HIF)-dependent mechanisms. Thus, PAH developed less often in murine models that were hemizygous for HIF1α and HIF2α[40, 41]. Activation of HIF resulting from down-regulation of prolyl hydroxylase domain-containing protein 2 (PHD2) has recently been shown to cause severe HIF2α-dependent PAH[15]. Efforts to elucidate downstream pathways involved in HIF2α-dependent PAH have included deletion of pulmonary endothelial Arg1, with resulting attenuation of PAH severity[13]. Importantly however, Arg2 is the major arginase isoform in endothelial cells, and Arg2 is selectively upregulated over Arg1 by hypoxia as shown in our current study and in previous work by other groups[8, 13, 41, 42]. Further investigation into hypoxia-mediated transcriptional regulation of Arg2 in pulmonary endothelial dysfunction and PAH is therefore warranted.

Our work demonstrates that KLF15 is a novel transcriptional regulator of Arginase 2 and describes the impact of this interaction in the context of hypoxia. Using ChIP and luciferase reporter assays for Arg2 promoter activity we have shown that KLF15 directly binds to the Arg2 promoter and represses its transcription (Figure 4). Hypoxia augmented Arg2 promoter

activity, but this upregulation was completely blocked by KLF15 overexpression. Hypoxia increased reactive oxygen species generation, and decreased NO production in HPMEC, and these effects were abrogated by increased expression of KLF15. Ectopic reconstitution of Arg2 blunted the protective effect of KLF15 on NO production, suggesting that Arg2 is a major effector target for KLF15 signaling in HPMEC.

Transcriptional repression of Arg2 by KLF15 is released in hypoxic conditions, as KLF15 is translocated to the cytoplasm by SENP1-mediated reversal of post-translational SUMO-1 conjugation to KLF15. A role for SENP1 in the regulation of responses to hypoxia has been described previously and the mechanism involves stabilization of HIF1α through decreased SUMO conjugation and ubiquitin-proteasome dependent degradation. In the current study, exposure of HPMEC to increasing concentrations of SENP1 shRNA produced dose-dependent effects on KLF15 conjugation, whereas overexpression of SENP1 had the reverse effect. SUMO conjugation is frequently required for nuclear localization, and SUMOylation also regulates nuclear retention of some proteins and transcription factors[43-45]. Interestingly, SUMOylation is known to be critical for nuclear localization of another Kruppel-Like Factor, KLF5. However, the SUMO conjugation site in KLF5 is not conserved in KLF15, and this suggests that the SUMOylation sites in these two KLF family members have distinct functions. Further, molecular activation of SENP1 (and hence deSUMOylation) by hypoxia has been shown to occur via the formation of an intermolecular disulfide bond between Cys 603 and Cys 613[46]. These observations are consistent with our findings that KLF15 is deSUMOylated and translocated to the cytoplasm from nucleus in response to hypoxia.

As mentioned above, our findings that the overall abundance of KLF15, as well as its nuclear location and stabilization is regulated by SUMO-1 in an oxygen-sensitive manner is not without precedent. HIF1α abundance and location is primarily regulated by hydroxylation, a process that is O_2-dependent and targets the protein for ubiquitination and proteosomal degradation (in hypoxic conditions, decreased hydroxylation stabilizes HIF1α and allows it to bind to HIF1β allowing transcription of hypoxia-driven target genes). However, emerging evidence suggest that SUMOylation of HIF1α regulates its activity and abundance. Indeed, Bae et al. demonstrated that SUMOylation of Lys391/Lys 477 increases its stability and enhances transcriptional activity by blocking HIF ubiquitination and proteasomal degradation[47]. Moreover, in the context of a rat hypoxic pulmonary hypertension model, Jiang, Y et al. showed that SUMO-1 seemed to stabilize HIF1α in response to hypoxia, and upregulated HIF1-regulated genes[48, 49]. Thus, in the context of both HIF1 and KLF15, SUMOylation mediated by SUMO-1 appears to stabilize the transcription factors. In the case of HIF1, increased SUMOylation is driven by hypoxia and leads to activation of hypoxia-sensitive genes. In contrast, for KLF15, hypoxia leads to destabilization of the transcriptional repression of the deleterious gene Arg2, and results in an increase in Arg2 transcription and downstream vascular endothelial dysfunction.

Tissue-specific function of KLF15 as an epigenetically and metabolically sensitive switch is another intriguing theme of the biology of this transcription factor that emerges from the experiments presented here. This is certainly in keeping with previous ground-breaking work from others in the field, indicating that KLF15 interaction with cell- and tissue-specific

nuclear targets causes alteration of cell fate or metabolism in response to autocrine signaling, growth factors, substrate availability, and diurnal cycling in at least four diverse contexts[50, 51]. KLF15 has been implicated in endothelin inhibition of Bone morphogenetic protein (BMP) endothelial cell precursor-derived regulator and downstream vasculogenesis[52]. Secondly, SMAD4 and the progesterone receptor trigger KLF15-mediated repression of uterine epithelial growth during mouse embryo implantation. Third, KLF15 interacts with a complex of the liver X receptor, retinoid X receptor, and RIP140 in the murine hepatocyte nucleus in the setting of fasting conditions to drive the transcriptional repression of SREBP-1c with a resulting increase in gluconeogenesis. Fourth, KLF15 has also recently been shown to mediate diurnal metabolic oscillation between catabolic and resting states in rodent cardiomyocytes via transcriptional activation and repression (respectively) of genes regulating ATP availability and other issues in cellular energetics. Our data showing that KLF15 mediates alteration of human pulmonary microvascular endothelial cell function as well as rat pulmonary artery responses in response to ambient oxygen is, therefore, in keeping with its function in other contexts - KLF15 is a master regulator of homeostatic function in response to environmental stimuli.

Finally, the current work addresses an urgent need for new therapeutic strategies in pulmonary hypertension[53]. This need has prompted the PH community to focus on genetic and epigenetic control of inflammation, aberrant growth control, and other sources of cellular dysfunction in the pulmonary circulation[54, 55]. The need for paradigm change in the conceptual framework underlying health care for pulmonary hypertension could be facilitated by strategies for the support of KLF15 levels in lung microvasculature via changes in the sensitivity of the SENP1 hypoxia response element, via protection of KLF15 SUMOylation, via inhibition of KLF15 interactions with SENP1, and/or via blocking KLF15 targeting for ubiquitin-mediated proteasomal clearance. Single and multimodal approaches to KLF15 preservation and augmentation need to be investigated during exposure to hypoxia, and to other environmental stressors that have been implicated in the pathogenesis of pulmonary hypertension - including altered estrogen metabolism, mitogen exposure, and oxidative stress. Indeed, endothelial responses and resulting vascular dysfunction in response to each of these perturbations have been shown to involve SUMOylation and/or deSUMOylation via SENP in models of other diseases. This constellation of data supports the notion that these pathways may be fruitful avenues of approach for pulmonary hypertension therapeutics as well[49, 56-60].

Supplementary Material

Refer to Web version on PubMed Central for supplementary material.

Acknowledgments

DISCLOSURES

We are grateful to Prof. Dr. Patrick MacDonald for the kind gift of GFP-SENP1 adenoviruses. We would like to thank Dr. Naz Paolocci for assistance with reactive oxygen measurements with EPR. We would like to acknowledge partial support for the statistical analysis from the National Center for Research Resources and the National Center for Advancing Translational Sciences (NCATS) of the National Institutes of Health through Grant Number 1UL1TR001079. The authors are also grateful to Andrea Wecker for technical assistance.

Source of Funding: This work was supported by an American Heart Association Scientist Development Grant and a Johns Hopkins University ACCM StAAR Investigator Award to Deepesh Pandey, NHLBI R01 HL124213 to Dan Berkowitz, and a grant from Kley Biomimetics to Lewis Romer.

References

1. Dunham-Snary KJ, Wu D, Sykes EA, Thakrar A, Parlow LR, Mewburn JD, Parlow JL, Archer SL. Hypoxic Pulmonary Vasoconstriction: From Molecular Mechanisms to Medicine. Chest. 2017; 151:181–192. [PubMed: 27645688]
2. Murata T, Sato K, Hori M, Ozaki H, Karaki H. Decreased endothelial nitric-oxide synthase (eNOS) activity resulting from abnormal interaction between eNOS and its regulatory proteins in hypoxia-induced pulmonary hypertension. J Biol Chem. 2002; 277:44085–92. [PubMed: 12185080]
3. Komai H, Naito Y, Aimi Y, Kimura H. Nitric oxide synthase expression in lungs of pulmonary hypertensive patients with heart disease. Cardiovasc Pathol. 2001; 10:29–32. [PubMed: 11343992]
4. Le Cras TD, Xue C, Rengasamy A, Johns RA. Chronic hypoxia upregulates endothelial and inducible NO synthase gene and protein expression in rat lung. Am J Physiol. 1996; 270:L164–70. [PubMed: 8772540]
5. Resta TC, Gonzales RJ, Dail WG, Sanders TC, Walker BR. Selective upregulation of arterial endothelial nitric oxide synthase in pulmonary hypertension. Am J Physiol. 1997; 272:H806–13. [PubMed: 9124442]
6. Xue C, Johns RA. Upregulation of nitric oxide synthase correlates temporally with onset of pulmonary vascular remodeling in the hypoxic rat. Hypertension. 1996; 28:743–53. [PubMed: 8901818]
7. Pandey D, Hori D, Kim JH, Bergman Y, Berkowitz DE, Romer LH. NEDDylation promotes endothelial dysfunction: a role for HDAC2. Journal of molecular and cellular cardiology. 2015; 81:18–22. [PubMed: 25655932]
8. Pandey D, Bhunia A, Oh YJ, Chang F, Bergman Y, Kim JH, Serbo J, Boronina TN, Cole RN, Van Eyk J, Remaley AT, Berkowitz DE, Romer LH. OxLDL triggers retrograde translocation of arginase2 in aortic endothelial cells via ROCK and mitochondrial processing peptidase. Circulation research. 2014; 115:450–9. [PubMed: 24903103]
9. Sikka G, Pandey D, Bhuniya AK, Steppan J, Armstrong D, Santhanam L, Nyhan D, Berkowitz DE. Contribution of arginase activation to vascular dysfunction in cigarette smoking. Atherosclerosis. 2013; 231:91–4. [PubMed: 24125417]
10. Pandey D, Romer L, Berkowitz DE. Arginase II: atherogenesis beyond enzyme activity. J Am Heart Assoc. 2013; 2:e000392. [PubMed: 23938287]
11. Lei W, He Y, Shui X, Li G, Yan G, Zhang Y, Huang S, Chen C, Ding Y. Expression and analyses of the HIF-1 pathway in the lungs of humans with pulmonary arterial hypertension. Mol Med Rep. 2016; 14:4383–4390. [PubMed: 27667582]
12. Huetsch JC, Suresh K, Bernier M, Shimoda LA. Update on novel targets and potential treatment avenues in pulmonary hypertension. Am J Physiol Lung Cell Mol Physiol. 2016; 311:L811–L831. [PubMed: 27591245]
13. Cowburn AS, Crosby A, Macias D, Branco C, Colaco RD, Southwood M, Toshner M, Crotty Alexander LE, Morrell NW, Chilvers ER, Johnson RS. HIF2alpha-arginase axis is essential for the development of pulmonary hypertension. Proceedings of the National Academy of Sciences of the United States of America. 2016; 113:8801–6. [PubMed: 27432976]
14. Krotova K, Patel JM, Block ER, Zharikov S. Hypoxic upregulation of arginase II in human lung endothelial cells. Am J Physiol Cell Physiol. 2010; 299:C1541–8. [PubMed: 20861464]
15. Kapitsinou PP, Rajendran G, Astleford L, Michael M, Schonfeld MP, Fields T, Shay S, French JL, West J, Haase VH. The Endothelial Prolyl-4-Hydroxylase Domain 2/Hypoxia-Inducible Factor 2 Axis Regulates Pulmonary Artery Pressure in Mice. Mol Cell Biol. 2016; 36:1584–94. [PubMed: 26976644]
16. Iyer NV, Kotch LE, Agani F, Leung SW, Laughner E, Wenger RH, Gassmann M, Gearhart JD, Lawler AM, Yu AY, Semenza GL. Cellular and developmental control of O2 homeostasis by hypoxia-inducible factor 1 alpha. Genes Dev. 1998; 12:149–62. [PubMed: 9436976]

17. Abe J, Berk BC. Novel mechanisms of endothelial mechanotransduction. Arterioscler Thromb Vasc Biol. 2014; 34:2378–86. [PubMed: 25301843]
18. Marin T, Gongol B, Chen Z, Woo B, Subramaniam S, Chien S, Shyy JY. Mechanosensitive microRNAs-role in endothelial responses to shear stress and redox state. Free Radic Biol Med. 2013; 64:61–8. [PubMed: 23727269]
19. Davies PF, Civelek M, Fang Y, Fleming I. The atherosusceptible endothelium: endothelial phenotypes in complex haemodynamic shear stress regions in vivo. Cardiovasc Res. 2013; 99:315–27. [PubMed: 23619421]
20. De Val S, Black BL. Transcriptional control of endothelial cell development. Dev Cell. 2009; 16:180–95. [PubMed: 19217421]
21. Chiu JJ, Chien S. Effects of disturbed flow on vascular endothelium: pathophysiological basis and clinical perspectives. Physiol Rev. 2011; 91:327–87. [PubMed: 21248169]
22. Atkins GB, Jain MK. Role of Kruppel-like transcription factors in endothelial biology. Circulation research. 2007; 100:1686–95. [PubMed: 17585076]
23. Sangwung P, Zhou G, Nayak L, et al. KLF2 and KLF4 control endothelial identity and vascular integrity. JCI Insight. 2017; 2:e91700. [PubMed: 28239661]
24. Atkins GB, Wang Y, Mahabeleshwar GH, Shi H, Gao H, Kawanami D, Natesan V, Lin Z, Simon DI, Jain MK. Hemizygous deficiency of Kruppel-like factor 2 augments experimental atherosclerosis. Circ Res. 2008; 103:690–3. [PubMed: 18757824]
25. Sharma N, Lu Y, Zhou G, Liao X, Kapil P, Anand P, Mahabeleshwar GH, Stamler JS, Jain MK. Myeloid Kruppel-like factor 4 deficiency augments atherogenesis in ApoE−/− mice-brief report. Arterioscler Thromb Vasc Biol. 2012; 32:2836–8. [PubMed: 23065827]
26. Shankman LS, Gomez D, Cherepanova OA, Salmon M, Alencar GF, Haskins RM, Swiatlowska P, Newman AA, Greene ES, Straub AC, Isakson B, Randolph GJ, Owens GK. Corrigendum: KLF4-dependent phenotypic modulation of smooth muscle cells has a key role in atherosclerotic plaque pathogenesis. Nat Med. 2016; 22:217.
27. Lu Y, Zhang L, Liao X, et al. Kruppel-like factor 15 is critical for vascular inflammation. J Clin Invest. 2013; 123:4232–41. [PubMed: 23999430]
28. Lu Y, Haldar S, Croce K, Wang Y, Sakuma M, Morooka T, Wang B, Jeyaraj D, Gray SJ, Simon DI, Jain MK. Kruppel-like factor 15 regulates smooth muscle response to vascular injury-brief report. Arterioscler Thromb Vasc Biol. 2010; 30:1550–2. [PubMed: 20508206]
29. Haldar SM, Lu Y, Jeyaraj D, et al. Klf15 deficiency is a molecular link between heart failure and aortic aneurysm formation. Sci Transl Med. 2010; 2:26ra26.
30. Liao X, Haldar SM, Lu Y, Jeyaraj D, Paruchuri K, Nahori M, Cui Y, Kaestner KH, Jain MK. Kruppel-like factor 4 regulates pressure-induced cardiac hypertrophy. J Mol Cell Cardiol. 2010; 49:334–8. [PubMed: 20433848]
31. Bround MJ, Wambolt R, Luciani DS, Kulpa JE, Rodrigues B, Brownsey RW, Allard MF, Johnson JD. Cardiomyocyte ATP production, metabolic flexibility, and survival require calcium flux through cardiac ryanodine receptors in vivo. J Biol Chem. 2013; 288:18975–86. [PubMed: 23678000]
32. Pandey D, Gratton JP, Rafikov R, Black SM, Fulton DJ. Calcium/calmodulin-dependent kinase II mediates the phosphorylation and activation of NADPH oxidase 5. Mol Pharmacol. 2011; 80:407–15. [PubMed: 21642394]
33. Alaiti MA, Orasanu G, Tugal D, Lu Y, Jain MK. Kruppel-like factors and vascular inflammation: implications for atherosclerosis. Curr Atheroscler Rep. 2012; 14:438–49. [PubMed: 22850980]
34. Berkowitz DE, White R, Li D, Minhas KM, Cernetich A, Kim S, Burke S, Shoukas AA, Nyhan D, Champion HC, Hare JM. Arginase reciprocally regulates nitric oxide synthase activity and contributes to endothelial dysfunction in aging blood vessels. Circulation. 2003; 108:2000–6. [PubMed: 14517171]
35. Ryoo S, Gupta G, Benjo A, Lim HK, Camara A, Sikka G, Lim HK, Sohi J, Santhanam L, Soucy K, Tuday E, Baraban E, Ilies M, Gerstenblith G, Nyhan D, Shoukas A, Christianson DW, Alp NJ, Champion HC, Huso D, Berkowitz DE. Endothelial arginase II: a novel target for the treatment of atherosclerosis. Circ Res. 2008; 102:923–32. [PubMed: 18309100]

36. Pandey D, Sikka G, Bergman Y, Kim JH, Ryoo S, Romer L, Berkowitz D. Transcriptional regulation of endothelial arginase 2 by histone deacetylase 2. Arteriosclerosis, thrombosis, and vascular biology. 2014; 34:1556–66.
37. Harding R, Hooper SB. Regulation of lung expansion and lung growth before birth. J Appl Physiol (1985). 1996; 81:209–24. [PubMed: 8828667]
38. Rodriguez JA. Interplay between nuclear transport and ubiquitin/SUMO modifications in the regulation of cancer-related proteins. Semin Cancer Biol. 2014; 27:11–9. [PubMed: 24704338]
39. Sehat B, Tofigh A, Lin Y, Trocme E, Liljedahl U, Lagergren J, Larsson O. SUMOylation mediates the nuclear translocation and signaling of the IGF-1 receptor. Sci Signal. 2010; 3:ra10. [PubMed: 20145208]
40. Brusselmans K, Compernolle V, Tjwa M, Wiesener MS, Maxwell PH, Collen D, Carmeliet P. Heterozygous deficiency of hypoxia-inducible factor-2alpha protects mice against pulmonary hypertension and right ventricular dysfunction during prolonged hypoxia. J Clin Invest. 2003; 111:1519–27. [PubMed: 12750401]
41. Yu AY, Shimoda LA, Iyer NV, Huso DL, Sun X, McWilliams R, Beaty T, Sham JS, Wiener CM, Sylvester JT, Semenza GL. Impaired physiological responses to chronic hypoxia in mice partially deficient for hypoxia-inducible factor 1alpha. J Clin Invest. 1999; 103:691–6. [PubMed: 10074486]
42. Xu W, Kaneko FT, Zheng S, Comhair SA, Janocha AJ, Goggans T, Thunnissen FB, Farver C, Hazen SL, Jennings C, Dweik RA, Arroliga AC, Erzurum SC. Increased arginase II and decreased NO synthesis in endothelial cells of patients with pulmonary arterial hypertension. FASEB J. 2004; 18:1746–8. [PubMed: 15364894]
43. Terui Y, Saad N, Jia S, McKeon F, Yuan J. Dual role of sumoylation in the nuclear localization and transcriptional activation of NFAT1. J Biol Chem. 2004; 279:28257–65. [PubMed: 15117942]
44. Johnson ES. Protein modification by SUMO. Annu Rev Biochem. 2004; 73:355–82. [PubMed: 15189146]
45. Salinas S, Briancon-Marjollet A, Bossis G, Lopez MA, Piechaczyk M, Jariel-Encontre I, Debant A, Hipskind RA. SUMOylation regulates nucleo-cytoplasmic shuttling of Elk-1. J Cell Biol. 2004; 165:767–73. [PubMed: 15210726]
46. Xu Z, Lam LS, Lam LH, Chau SF, Ng TB, Au SW. Molecular basis of the redox regulation of SUMO proteases: a protective mechanism of intermolecular disulfide linkage against irreversible sulfhydryl oxidation. FASEB J. 2008; 22:127–37. [PubMed: 17704192]
47. Bae SH, Jeong JW, Park JA, Kim SH, Bae MK, Choi SJ, Kim KW. Sumoylation increases HIF-1alpha stability and its transcriptional activity. Biochem Biophys Res Commun. 2004; 324:394–400. [PubMed: 15465032]
48. Jiang Y, Wang J, Tian H, Li G, Zhu H, Liu L, Hu R, Dai A. Increased SUMO-1 expression in response to hypoxia: Interaction with HIF-1alpha in hypoxic pulmonary hypertension. Int J Mol Med. 2015; 36:271–81. [PubMed: 25976847]
49. Cheng J, Kang X, Zhang S, Yeh ET. SUMO-specific protease 1 is essential for stabilization of HIF1alpha during hypoxia. Cell. 2007; 131:584–95. [PubMed: 17981124]
50. Takeuchi Y, Yahagi N, Aita Y, et al. KLF15 Enables Rapid Switching between Lipogenesis and Gluconeogenesis during Fasting. Cell Rep. 2016; 16:2373–86. [PubMed: 27545894]
51. Zhang L, Prosdocimo DA, Bai X, Fu C, Zhang R, Campbell F, Liao X, Coller J, Jain MK. KLF15 Establishes the Landscape of Diurnal Expression in the Heart. Cell Rep. 2015; 13:2368–2375. [PubMed: 26686628]
52. Helbing T, Volkmar F, Goebel U, Heinke J, Diehl P, Pahl HL, Bode C, Patterson C, Moser M. Kruppel-like factor 15 regulates BMPER in endothelial cells. Cardiovascular research. 2010; 85:551–9. [PubMed: 19767294]
53. Gurtu V, Michelakis ED. A Paradigm Shift Is Needed in the Field of Pulmonary Arterial Hypertension for Its Entrance Into the Precision Medicine Era. Circulation research. 2016; 119:1276–1279. [PubMed: 27932471]
54. Negi V, Chan SY. Discerning functional hierarchies of microRNAs in pulmonary hypertension. JCI Insight. 2017; 2:e91327. [PubMed: 28289720]

55. Gamen E, Seeger W, Pullamsetti SS. The emerging role of epigenetics in pulmonary hypertension. Eur Respir J. 2016; 48:903–17. [PubMed: 27492834]

56. Anbalagan M, Huderson B, Murphy L, Rowan BG. Post-translational modifications of nuclear receptors and human disease. Nucl Recept Signal. 2012; 10:e001. [PubMed: 22438791]

57. Heo KS, Chang E, Le NT, Cushman H, Yeh ET, Fujiwara K, Abe J. De-SUMOylation enzyme of sentrin/SUMO-specific protease 2 regulates disturbed flow-induced SUMOylation of ERK5 and p53 that leads to endothelial dysfunction and atherosclerosis. Circulation research. 2013; 112:911–23. [PubMed: 23381569]

58. Chang E, Abe J. Kinase-SUMO networks in diabetes-mediated cardiovascular disease. Metabolism. 2016; 65:623–33. [PubMed: 27085771]

59. Ferdaoussi M, Dai X, Jensen MV, et al. Isocitrate-to-SENP1 signaling amplifies insulin secretion and rescues dysfunctional beta cells. J Clin Invest. 2015; 125:3847–60. [PubMed: 26389676]

60. Dai XQ, Plummer G, Casimir M, Kang Y, Hajmrle C, Gaisano HY, Manning Fox JE, MacDonald PE. SUMOylation regulates insulin exocytosis downstream of secretory granule docking in rodents and humans. Diabetes. 2011; 60:838–47. [PubMed: 21266332]

Highlights

- Regulation of genes that mediate hypoxia-induced blood vessel dysfunction is an important topic for critical care and regenerative medicine.
- We demonstrate that deleterious effects of hypoxia on pulmonary vascular endothelium are mediated by impairment of upregulation of protective genes and down regulation of injurious genes that govern endothelial function by the transcription factor Kruppel Like Factor 15 (KLF15). We studied the effect of KLF15 on the transcriptional regulation of the enzyme, Arginase 2 - a gene known to downregulate the function of eNOS through substrate competition. We demonstrate that KLF15 is a trans-repressor of Arginase 2 in pulmonary microvascular endothelial cells. Hypoxia leads to a decrease in the available pool of KLF15 and an increase in the transcription of Arginase 2.
- We further showed that hypoxia reduces the abundance of KLF15 by a post-translational modification that involves SUMO-1 and SENP1. This modification leads to KLF15 translocation from the nucleus to the cytoplasm, and to KLF15 clearance by ubiquitin-mediated proteasomal degradation.
- Our finding that KLF15 is a critical regulator of pulmonary endothelial function and dysfunction in hypoxia has important implications for therapy in pulmonary vascular diseases.

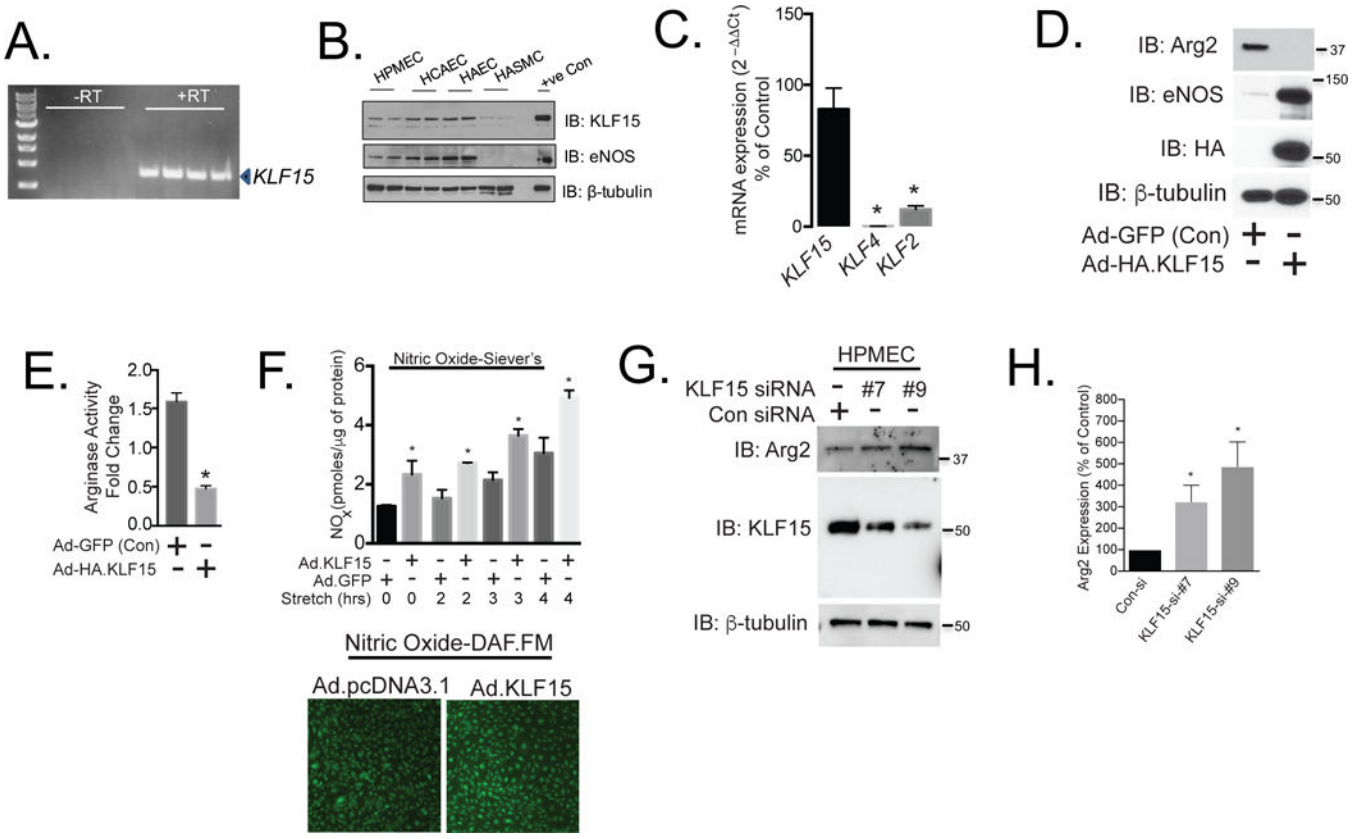

Figure 1. KLF15 is the major Kruppel-Like Factor in HPMEC and important regulator of critical endothelial enzymes- Arginase 2 and eNOS

Total RNA from Human Pulmonary Microvascular endothelial cells was converted to cDNA and the relative mRNA expression of KLF15 was determined in quiescent HPMEC using real-time PCR (N=3), B) Cell lysates from HPMEC, human coronary artery endothelial cells (HCAEC), Human Aortic Endothelial Cells (HAEC), Human Aortic Smooth Muscle Cells (HASMC) were subjected to western blotting with KLF15, eNOS and β-tubulin antibodies (N=4). Cell lysates from HPMEC overexpressing HA-KLF15 was used as a positive control, C) Total RNA from Human Pulmonary Microvascular endothelial cells was converted to cDNA and the relative mRNA expression of KLF2, 4 and 15 was determined in quiescent HPMEC using real-time PCR (N=3) *p<0.05 vs *KLF15* expression level. D) Lysates of HPMEC with transient overexpression of adenovirally transduced HA-tagged KLF15 or GFP (control) were subjected to immunoblotting with antibodies against Arginase 2 (Arg2), eNOS, HA and β-tubulin (N=4). E) Arginase activity was assayed in lysates of HPMEC expressing either GFP (control) or HA-KLF15 (N=6) *p<0.05 vs control (Ad.GFP). F) Media from cultures of HPMEC expressing either GFP (control) or HA-KLF15 was collected at 2, 3, and 4 hours of non-stretch or cyclic stretch conditions, and nitric oxide levels were measured using a Siever's NO analyzer (N=3) *p<0.05 vs control (Ad.GFP and no stretch). DAF-DA fluorescence of HPMEC overexpressed with either GFP (control) or KLF15(F, lower panel) (N=3). G) HPMEC were transfected with either scrambled siRNA or KLF15 siRNA directed to the CDS region of KLF15 (#7 and #9; Qiagen Flexitube) for 48

hours and cell lysates were subjected to immunoblotting with anti- Arg2, -KLF15 and β-tubulin antibodies (N=3) *p<0.05 vs Con siRNA.

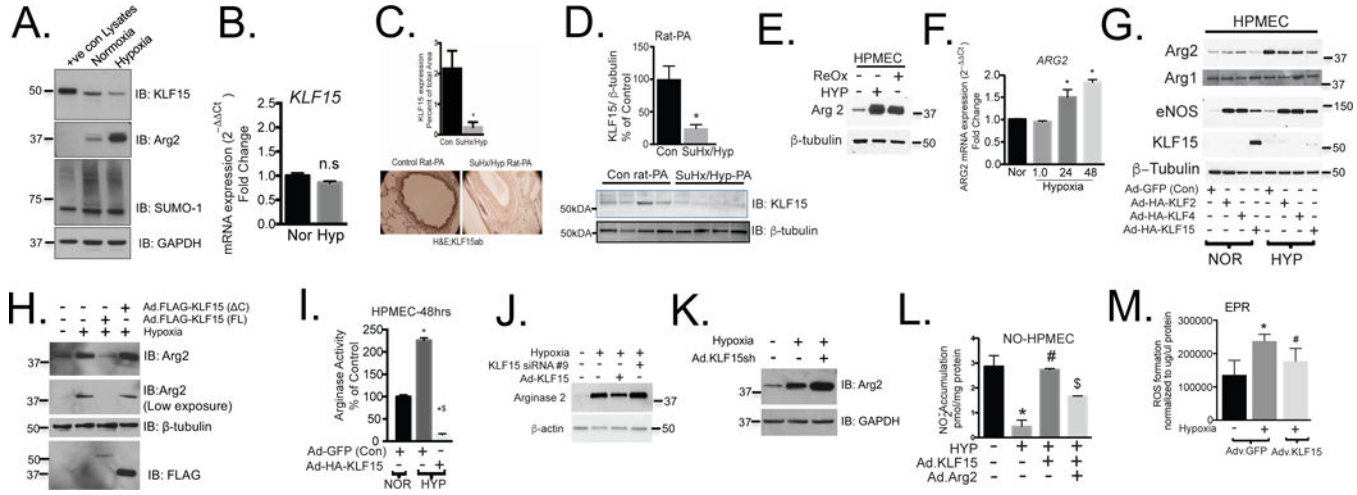

Figure 2. KLF15 is a novel downstream target of hypoxia and its increased expression reverses hypoxia-mediated increases in Arginase 2 expression and ROS generation, and decreased Nitric Oxide production in HPMEC

A) Cell lysates from HPMEC exposed to hypoxia (2% O_2) for 24 hours were subjected to western blotting with KLF15, Arg2 and GAPDH antibodies (N=4). Cell lysates from HPMEC overexpressing HA-KLF15 was used as a positive control. B) KLF15 mRNA levels were determined by real time PCR from HPMEC exposed to hypoxia (2% O_2) for 24 hours (N=3) $^{n.s}p>0.05$ vs normoxia. Pulmonary artery from rats subjected to either control or sugen-hypoxia protocol was C) subjected to immunohistochemical staining with KLF15 antibodies and D) immunoblotted with KLF15 and beta tubulin antibodies*$p<0.05$ vs control (without sugen hypoxia). E) HPMEC were exposed to hypoxia (2% O_2) for 24 hours, followed by reoxygenation (21%) for 24 hours. Cell lysates were subjected to immunoblotting with antibodies against Arg2 and β-tubulin (N=4). F) HPMEC were exposed to hypoxia (2% O_2) for 1, 24 or 48 hours and Arg2 mRNA levels were determined by real time PCR (N=3) *$p<0.05$ vs normoxia. G) HPMEC with adenovirally mediated overexpression of GFP, KLF2, KLF4, or KLF15 were exposed to either hypoxia or normoxia for 24 hours and immunoblotted using antibodies against Arg2, Arg1, eNOS, KLF15 and β-tubulin (N=4). H) Effect of overexpression of either full-length KLF15 or C-terminal truncated KLF15 were determined in hypoxia induced Arg2 levels (N=4) I) HPMEC cells expressing either GFP (control) or KLF15 were subjected to normoxia or hypoxia and arginase activity was determined in the cell lysates (N=6) *$p<0.05$ vs normoxia and $^{\$}p<0.05$ vs GFP overexpressed HPMEC exposed to normoxia. J&K) Quiescent HPMEC expressing GFP (control) were subjected to either normoxia or hypoxia. Additionally, HPMEC with either (J) transfected siRNA (#9) or (K) adenoviral mediated transient knockdown of KLF15 with shRNA were exposed to hypoxia for 24 hours and cell lysates were subjected to immunoblotting with Arg2 and β-tubulin (N=3). L) HPMEC expressing GFP were kept in normoxic conditions and HPMEC expressing GFP, KLF15, or KLF15 + Arg2 were exposed to hypoxic conditions. After 24 hours of hypoxia, cell culture media was collected and subjected to nitrite measurements using Siever's NO analyzer (N=3) *$p<0.05$ vs normoxia, $^{\#}p<0.05$ vs hypoxia and $^{\$}p<0.05$ vs KLF15 overexpressed HPMEC exposed to hypoxia. M) Lysates from HPMEC expressing GFP or KLF15, and in normoxic or hypoxic conditions for 24 hours were analyzed for levels of reactive oxygen species using EPR

(N=3) *p<0.05 vs normoxia and #p<0.05 vs GFP overexpressed HPMEC exposed to hypoxia.

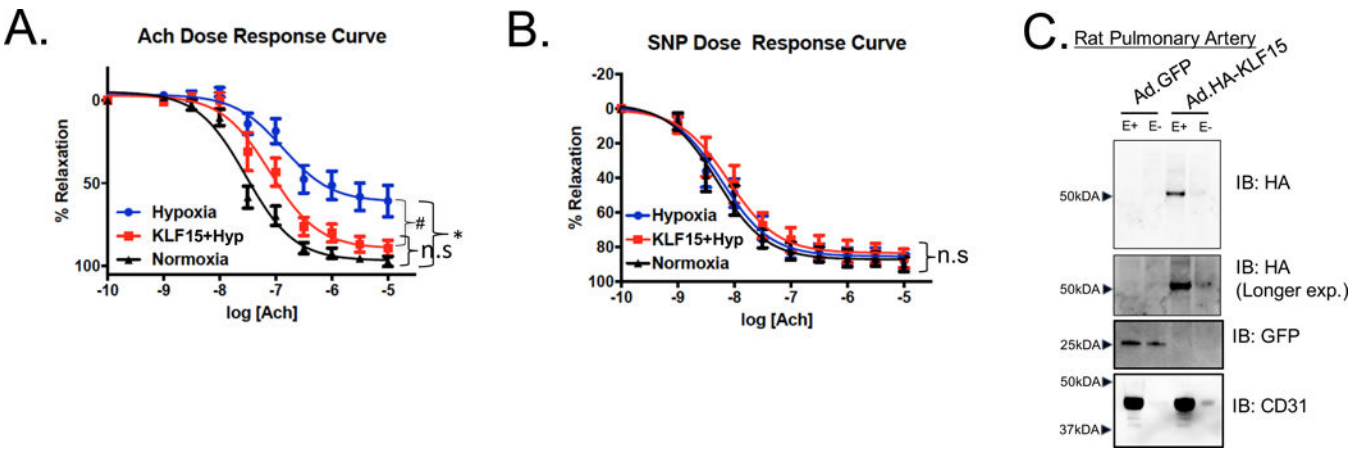

Figure 3. KLF15 provides protection against hypoxia-induced endothelial dysfunction

A and B) Isolated rat pulmonary arteries, transduced with 100 MOI of either GFP or KLF15 adenovirus, were exposed to normoxia or hypoxia. (A) Acetylcholine (ACh)- and (B) and sodium nitroprusside (SNP)-mediated relaxation was measured in arteries precontracted with phenylephrine by wire force tension myography. C) 48 hrs post transduction of isolated pulmonary arteries with either Ad. Empty pcDNA3.1 vector (control) or Ad. HA-KLF15 in endothelial growth media endothelium denuded (E-) and endothelium intact (E+) PA segments were subjected to snap freezing in liquid nitrogen and immunoblotted with HA, GFP and CD31 (endothelial marker). (N=8-10) *$p<0.05$ vs normoxia with Ach doses 10^{-7}, 10^{-6} and 10^{-5} and $^{\#}p<0.05$ vs hypoxia with all doses of SNP.

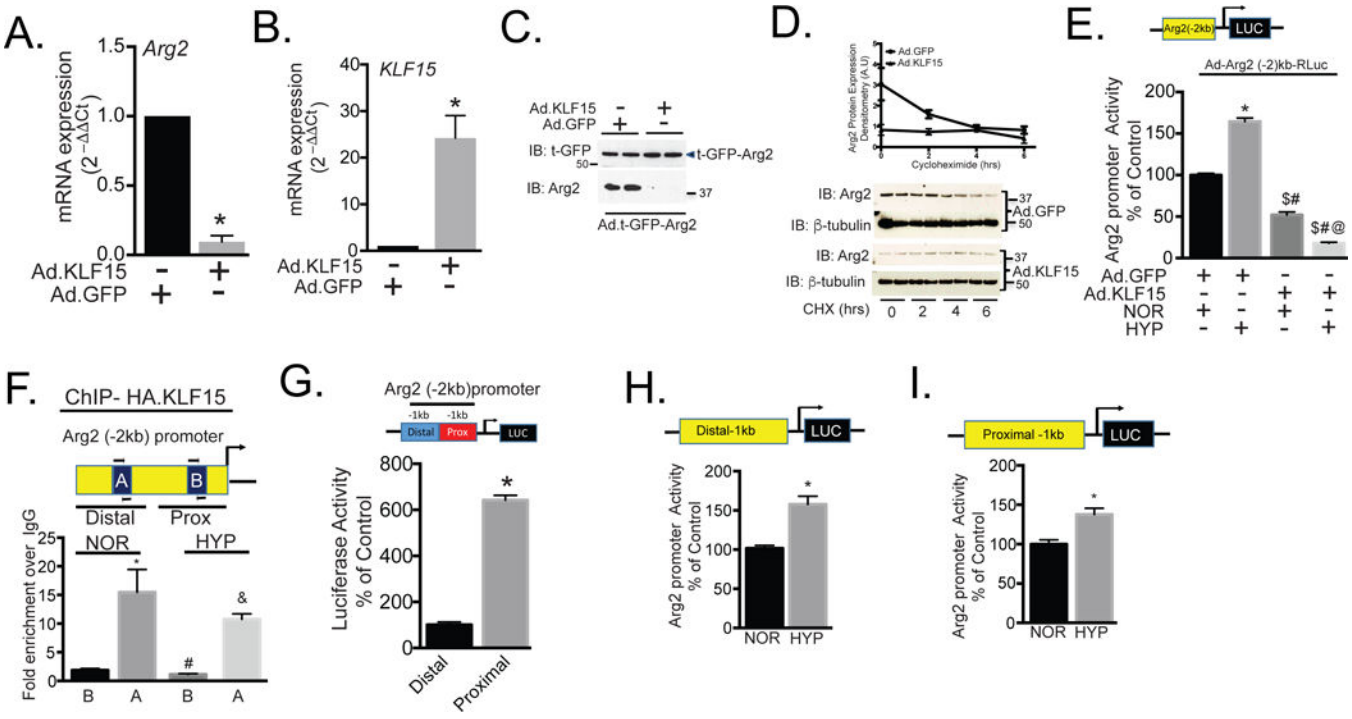

Figure 4. KLF15 regulates Arg2 transcription in HPMEC via direct interaction with the proximal portion of the Arg2 promoter

HPMEC overexpressing either GFP or KLF15 were subjected to RT-PCR and mRNA expression was determined using specific primers for A) Arg2 or B) KLF15, and 18s (N=3) *p<0.05 vs GFP (control) overexpressed HPMEC. C) turbo-GFP tagged Arg2 was co-expressed in HPMEC with either GFP or KLF15 and the cell lysates were subjected to immunoblotting with either t-GFP or Arg2 antibodies (N=4). D) HPMEC overexpressing either GFP or KLF15 were subjected to a cycloheximide (25μg/mL) chase protocol and cell lysates were subjected to immunoblotting with Arg2 and ß-tubulin antibodies at 0, 2, 4 and 6 hours after cycloheximide (N=3). E) HPMEC co-expressing an Arg2-2kb promoter-luciferase reporter construct (shown at the top of the panel) with either KLF15 or GFP were exposed to either normoxic or hypoxic conditions and cell lysates were subjected to firefly luciferase activity assay (promega's Dual-Glo luciferase kit) (N=3) *p<0.05 vs GFP overexpressed normoxia exposed HPMEC, $p<0.05 GFP overexpressed hypoxia exposed HPMEC, #p<0.05 vs GFP overexpressed normoxia exposed HPMEC and @p<0.05 vs KLF15 overexpressed normoxia exposed HPMEC. Renilla luciferase activity from a receptor tyrosine kinase (RTK) promoter adenoviral construct was used as a normalization control. F) HPMEC overexpressing HA-KLF15, and exposed to either normoxia or hypoxia were subjected to a ChIP assay. HA antibody and primers spanning the specific regions of Arg2 promoter indicated as A and B were used in the PCR reaction (N=3) *p<0.05 vs arg2 promoter region #B in normoxic condition, #p<0.05 vs arg2 promoter region #A in normoxic condition and &p<0.05 vs arg2 promoter region #B in hypoxic condition. G) Firefly luciferase chemiluminescence was determined in quiescent HPMEC expressing a Arg2-1kb promoter-luciferase reporter construct that was either 1kb proximal or distal to the transcription start site. Renilla luciferase activity from an RTK promoter adenoviral construct was used as a normalization control. H-I) HPMEC expressing a Arg2-1kb

promoter-luciferase reporter construct that was either 1kb proximal or distal to the transcription start site were exposed to normoxic or hypoxic conditions (24h) and cell lysates were subjected to firefly luciferase activity assay (promega's Dual-Glo luciferase kit) *p<0.05 vs distal region of Arg2-2kb promoter. Renilla luciferase activity from RTK promoter adenoviral construct was used as a normalization control. [N=3 for all luciferase activity experiments] *p<0.05 vs normoxia.

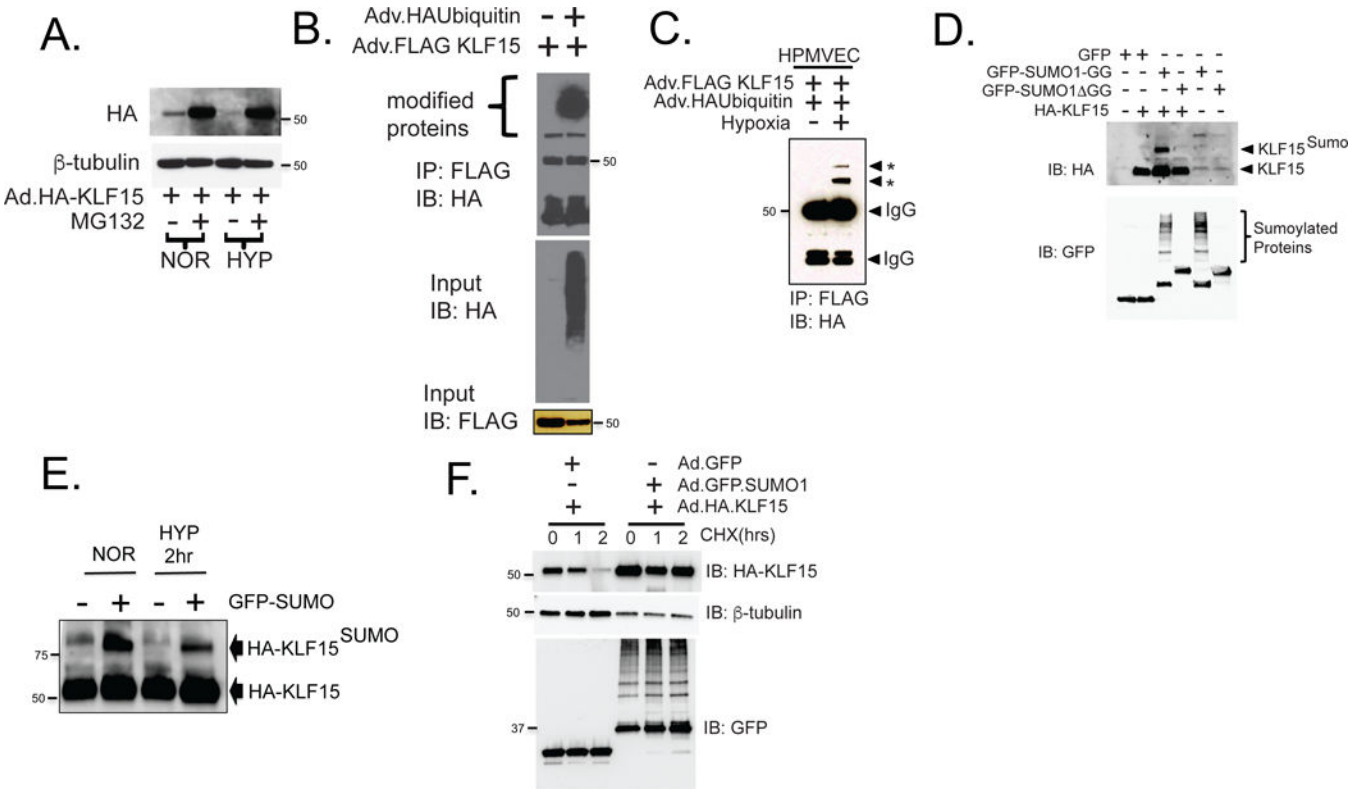

Figure 5. Hypoxia downregulates KLF15 levels in HPMEC via enhanced ubiquitin mediated proteasomal clearance and SUMO-1 mediated reduced protein stability

A) HPMEC expressing HA-tagged KLF15 were subjected to normoxia or hypoxia with or without MG132 (0.5μM) for 24 hours, and cell lysates were immunoblotted with HA antibody (N=4). B) Lysates from HPMEC co-expressing FLAG-KLF15 and either GFP or HA-ubiquitin were subjected co-immunoprecipitation experiments with anti-FLAG antibody and immunoblotted with anti-HA antibody (N=4). C) The experimental conditions described in B, above, were executed in normoxia or hypoxia (24h). D) Lysates from HPMEC that were co-expressing HA-KLF15 and either GFP, GFP-SUMO1-active, or GFP-SUMO1-inactive, or GFP-SUMO1-active or GFP-SUMO1-inactive alone, were immunoblotted with anti-HA and anti-GFP antibodies (N=4). E) Lysates from HPMEC exposed to normoxia or hypoxia while co-expressing either HA-KLF15 and GFP, or HA-KLF15 and GFP SUMO1-active were immunoblotted with anti-HA, and anti-GFP antibodies (N=4). F) HPMEC co-expressing HA-KLF15 and either GFP or GFP SUMO1-active were treated with 25 μg/mL of cycloheximide (CHX) and cell lysates were harvested after 1hr and 2hr of treatment followed by western blotting with anti-HA and anti-ß-tubulin antibodies (N=3).

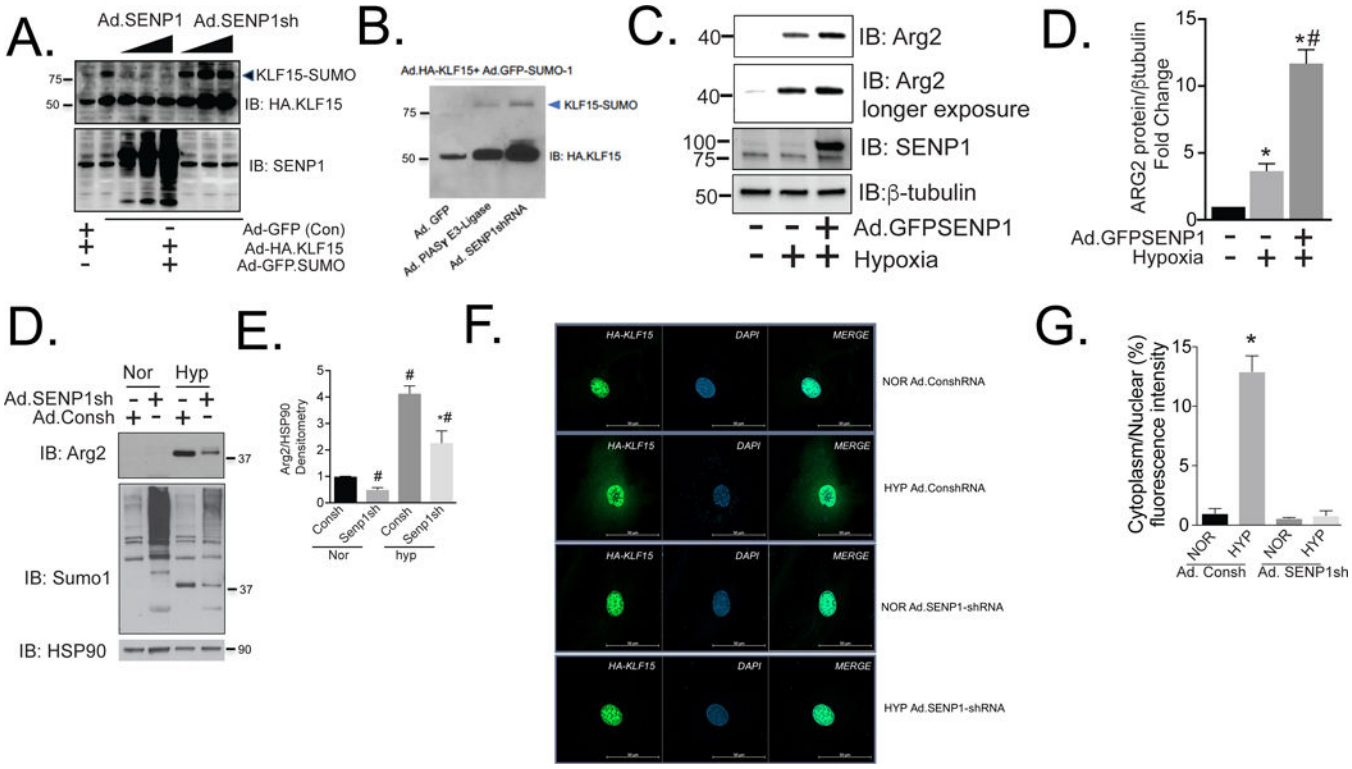

Figure 6. SENP1 mediates hypoxia induced Arg2 expression that involves translocation of KLF15 from nucleus to cytoplasm

A HPMEC co-transduced with either 1) HA-KLF15, GFP-SUMO1 and GFP (control), or 2) HA-KLF15, GFP-SUMO1 and increasing concentrations of GFP-SENP1 cDNA, or 3) HA-KLF15, GFP-SUMO1 and increasing concentration of SENP1 shRNA adenoviruses were cultured in normoxic or hypoxic conditions for 24 hours and cell lysates were immunoblotted with HA antibody (N=4). B) HPMEC expressing either PIASγ E3 ligase or SENP1shRNA were co transduced with either HA-KLF15 and GFP or HA-KLF15 and GFP-SUMO-1 and cell lysates were subjected to western blotting with HA antibodies (N=4). C) HPMEC expressing either GFP or GFP tagged SENP1 is exposed to normoxia or hypoxia and cell lysates were immunoblotted with Arg2, SENP1 and -β-tubulin antibodies (N=4). D) Densitometry analysis for (C) *p<0.05 vs normoxia exposed HPMEC and $^{\#}$p<0.05 vs hypoxia exposed HPMEC. E) HPMEC transduced with either control shRNA or SENP1shRNA were subjected to normoxia or hypoxia and cell lysates were subjected to western blotting with Arg2, SUMO-1 and HSP90 (loading control) antibodies (N=4). E) Densitometry analysis for (D) $^{\#}$p<0.05 vs normoxia exposed control shRNA transfected HPMEC and *p<0.05 vs hypoxia exposed control shRNA transfected HPMEC. F) HPMEC subjected to adenoviral co-transduction with either control shRNA and HA-KLF15 or SENP1shRNA and HA-KLF15 were exposed to either normoxic or hypoxic conditions for 24 hours and prepared for epifluorescence analysis by fixation with 3.7% paraformaldehyde, and labeling with anti-HA primary antibody and anti-rat alexa 465 secondary antibody (N=3). Images were acquired using a confocal microscope (Zeiss LSM 800 laser-scanning). G) Quantification of fluorescent intensity for (F) presented as a ratio of cytoplasm and

nucleus fluorescent intensity *p<0.05 vs control shRNA transfected HPMEC exposed to normoxic conditions.

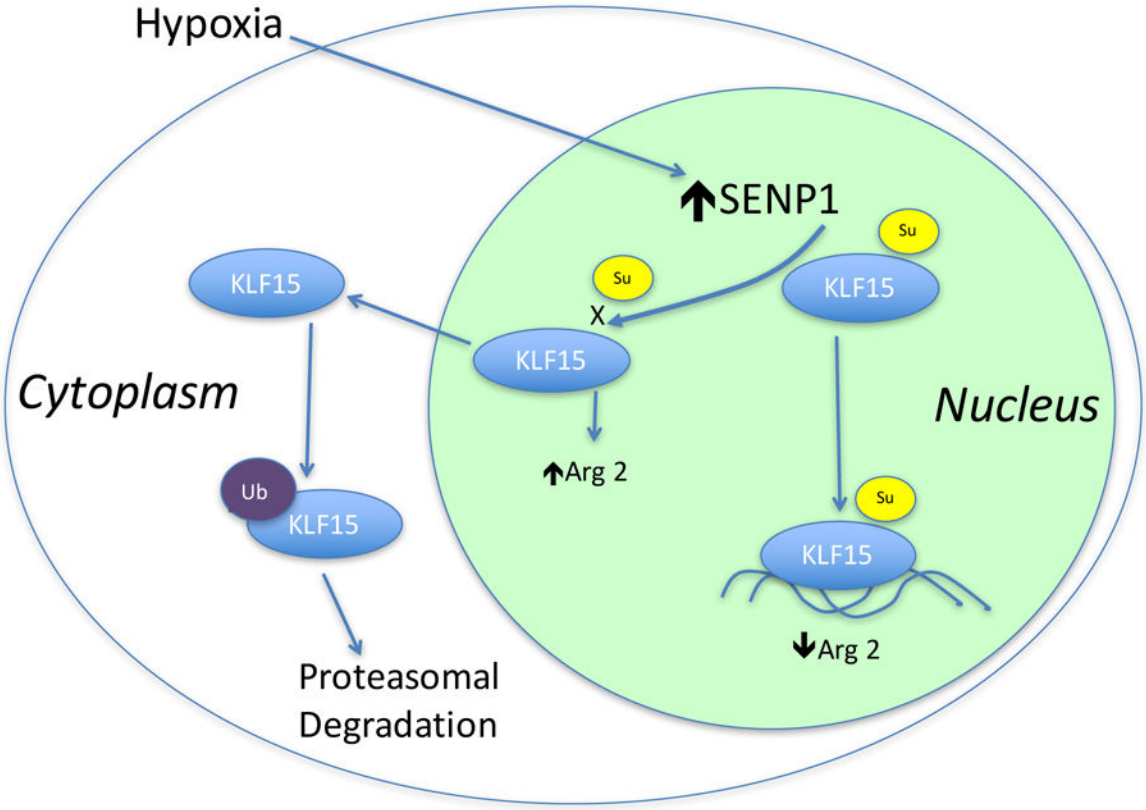

Figure 7. Schematic of pathways studied in current study

Pathway for KLF15 modulation of endothelial Arg2 and resulting pulmonary vascular endothelial dysfunction. Hypoxia downregulates KLF15 expression via ubiquitin proteasome system (UPS)- and SUMO/SENP1-mediated processes that leads to transcriptional upregulation of Arg2, reduction in eNOS function leading to pulmonary microvascular endothelial dysfunction. The role of hypoxia inducible factors (HIF1/HIF2) in KLF15 regulation by hypoxia is currently unknown.